J|A|C|S
ARTICLES
Published on Web 08/04/2006

Catalytic Polymerization and Facile Grafting of Poly(furfuryl alcohol) to Single-Wall Carbon Nanotube: Preparation of Nanocomposite Carbon

Bo Yi,[‡] Ramakrishnan Rajagopalan,[§] Henry C. Foley,*[,†,‡,§] Un Jeong Kim,[||,⊥] Xiaoming Liu,[||] and Peter C. Eklund[§,||]

Contribution from the Department of Chemistry, Department of Chemical Engineering, Materials Research Institute, and Department of Physics, Pennsylvania State University, University Park, Pennsylvania 16802

Received May 26, 2006; E-mail: hcf2@psu.edu

Abstract: A nanocomposite carbon was prepared by grafting a carbonizable polymer, poly(furfuryl alcohol) (PFA), to a single-wall carbon nanotube (SWNT). The SWNT was first functionalized with arylsulfonic acid groups on the sidewall via a method using a diazonium reagent. Both Raman and FTIR spectroscopies were used to identify the functional groups on the nanotube surface. HRTEM imaging shows that the SWNT bundles are exfoliated after functionalization. Once this state of the SWNTs was accomplished, the PFA-functionalized SWNT (PFA-SWNT) was prepared by in situ polymerization of furfuryl alcohol (FA). The sulfonic acid groups on the surface of the SWNT acted as a catalyst for FA polymerization, and the resulting PFA then grafted to the SWNTs. The surfaces of the SWNTs converted from hydrophilic to hydrophobic when they were wrapped with PFA. The formation of the polymer and the attraction between it and the sulfonic acid groups were confirmed by IR spectra. A nanocomposite carbon was generated by heating the PFA-SWNT in argon at 600 °C, a process during which the PFA was transformed to nanoporous carbon (NPC) and the sulfonic acid groups were cleaved from the SWNT. Based upon the Raman spectra and HRTEM images of the composite, it is concluded that SWNTs survive this process and a continuous phase is formed between the NPC and the SWNT.

Introduction

The discovery of carbon nanotubes (CNTs),[1] especially single-wall carbon nanotubes (SWNTs),[2] led to a new era of carbon science and technology which has sought a deeper understanding of their physics and chemistry while also exploring their potential for novel applications. The CNTs exhibit exceptional electronic and mechanical properties,[3,4] which make them attractive candidates as constituents of new high performance composites. Carbon/carbon (CC) composites are an important class of materials with applications in aerospace, the nuclear industry, and the chemical industry. In CC composites, the carbon fibers with their high mechanical strength are used to reinforce the brittle carbon matrix material. The fibers' mechanical properties determine, to a large extent, the strength and stiffness of the composite materials.[5] Due to the extraordinary properties of SWNTs, it would be interesting to augment or replace carbon fibers with SWNTs in CC composites to create a nanocomposite.[6] On the other hand, although a wide range of host materials have been explored for the preparation of CNT composites, including polymers,[7] ceramics,[8] metal,[9] and colloidal dispersions,[10] CNT composites made with carbon as the host material have been only rarely reported.[11] A feasible way to prepare a SWNT−carbon nanocomposite would be to disperse the SWNTs in a carbon precursor, for example, a carbonizable polymer. As such, poly(furfuryl alcohol) (PFA) is a good candidate for this purpose, since by heat treating PFA in inert

† Department of Chemistry.
‡ Department of Chemical Engineering.
§ Materials Research Institute.
|| Department of Physics.
⊥ Current address: Nano Fabrication Technology Center, Samsung Advanced Institute of Technology, Kyeongki-Do 449-712, Korea.

(1) (a) Oberlin, A.; Endo, M.; Koyama, T. *J. Cryst. Growth* **1976**, *32*, 335−349. (b) Iijima, S. *Nature* **1991**, *354*, 56−58.
(2) (a) Iijima S.; Ichihashi, T. *Nature* **1993**, *383*, 603−605. (b) Bethune, D. S.; Klang, C. H.; de Vries, M. S.; Gorman, G.; Savoy, R.; Vazquez, J.; Beyers, R. *Nature* **1993**, *383*, 605−607.
(3) Tans, S. J.; Devoret, M. H.; Dai, H.; Thess, A.; Smalley, R. E.; Geerlings, L. J.; Dekker, C. *Nature* **1997**, *386*, 474−477.
(4) Treacy, M. M. J.; Ebbesen, T. W.; Gibson, J. M. *Nature* **1996**, *381*, 678−680.
(5) Buckley, J. D.; Edie, D. D. *Carbon−carbon materials and composites*; Noyes Publications: 1993.
(6) Wagner, H. D.; Lourie, O.; Feldman, Y.; Tenne, R. *Appl. Phys. Lett.* **1998**, *72*, 188−190.
(7) (a) Shaffer, M. S. P.; Windle, A. H. *Adv. Mater.* **1999**, *11*, 937−941. (b) Jia, Z. J.; Wang, Z. Y.; Xu, C. L.; Liang, J.; Wei, B. Q.; Wu, D. H. Zhu, S. W. *Mater. Sci. Eng., A* **1999**, *271*, 395−400. (c) Kymakis, E.; Amaratunga, G. A. J. *Appl. Phys. Lett.* **2004**, *80*, 112−114. (d) Pirlot, C.; Willems, I.; Fonseca, A.; Nagy, J. B.; Delhalle, J. *Adv. Eng. Mater.* **2002**, *4*, 109−114. (e) Tang, B. Z.; Xu, H. *Macromolecules* **1999**, *32*, 2569−2576. (f) Niyogi, S.; Hamon, M. A.; Perea, D. E.; Kang, C. B.; Zhao, B.; Pal, S. K.; Wyant, A. E.; Itkis, M. E.; Haddon, R. C. Ultrasonic dispersions of SWNTs. *J. Phys. Chem. B* **2003**, *107*, 8799−8804.
(8) Hwang, G. L.; Hwang, K. C. *J. Mater. Chem.* **2001**, *11*, 1722−1725.
(9) (a) Kuzumaki, T.; Miyazawa, K.; Ichinose, H.; Ito, K. *J. Mater. Res.* **1998**, *13*, 2445−2449. (b) Dong, S. R.; Tu, J. P.; Zhang, X. B. *Mater. Sci. Eng., A* **2001**, *313*, 83−87.
(10) Jiang, L. Q.; Gao, L.; Sun, J. *J. Colloid Interface Sci.* **2003**, *260*, 89−94.
(11) Andrew, R.; Jacques, D. Rao, A. M.; Rantell, T.; Derbyshire, F.; Chen, Y.; Chen, J.; Haddon, R. C. *Appl. Phys. Lett.* **1999**, *75*, 1329−1331.

gas one obtains a nanoporous carbon (NPC) with a narrow pore size distribution (median around 0.5 nm).[12] Depending upon how this carbon is post-treated, it can be further densified or made to be highly porous. Therefore, it can be used for a range of potential applications, from those in which it is a structural component to those in which it is an adsorbent, gas separation membrane, catalyst support, or even an ultracapacitor.[13−16] Hence the combination of the NPC with SWNTs could lead to a nanocomposite with very interesting properties that could be tuned for different applications.

However, before that potential can be explored, let alone realized, the main challenge to progress in making such a nanocomposite of this kind (or any kind) with SWNTs is to overcome the poor dispersion and low interaction of SWNTs with the matrix or its precursor.[11,17−19] One reason for poor dispersion in monomers or polymers lies in the fact that the as-produced SWNTs are self-assembled in bundles with relatively strong interaction energies between neighboring tubes (∼0.5 eV/nm along the tube-to-tube contact length).[20,21] This, plus their inherent nonpolarity, makes it difficult to dissolve SWNTs either in water or in most organic solvents or to disperse them in most polymeric hosts. Therefore, our inability to manipulate and process SWNTs by methods used to make other composites has slowed progress in preparing new nanocomposites. But some work has been done within the constraints of solubility and dispersion imposed by the properties of the native SWNTs.[22−24]

Liquid-phase dispersion is often used to fabricate nanotube-polymer composites, and the most common method used to disperse SWNTs in a polymer is to suspend the tubes in a solvent containing the polymer and then to ultrasonicate the mixture.[7c,7d,11,25,26] Although this is easy and readily done, it is of limited value as a general method of nanocomposite preparation since precipitation and settling of the SWNTs occurs almost immediately after sonication is discontinued. Nonetheless, by dispersing the SWNTs in monomer (with or without ultrasonication) followed by rapid in situ polymerization polymer-SWNT nanocomposites have been made.[7b,e,27,28] However, a homogeneous dispersion within the polymer of the SWNTs is far from guaranteed due to their inherent insolubility. To approach a more uniform dispersion, the SWNTs should be modified to make their surfaces more compatible with the polymer matrix. It is commonly agreed that the nanotubes decorated with polymers that are structurally similar to the polymer should have good compatibility and would lead to much better nanocomposites.[29] Therefore to prepare a well-developed SWNT/NPC composite, we would prefer to disperse the SWNTs in furfuryl alcohol, then polymerize to form a polymer around the tubes, and then pyrolyze to create a strong carbon−carbon interface between the SWNTs and the NPC. Thus, the essential goal is to define a methodology that could enable SWNTs to disperse well in PFA by actually decorating them with PFA.

Recently, modification of SWNTs with polymers has been widely studied with the ultimate purpose of controlling their solubility and processibility, either through covalent bonding or noncovalent bonding. Smalley et al. reported that SWNTs could be reversibly wrapped with a variety of linear polymers such as poly(vinylpyrrolidone) (PVP) and polystyrene sulfonate (PSS).[30] Polysaccharides, such as starch and gum Arabic, were also able to exfoliate bundles and wrap individual SWNTs to make them soluble in water.[31,32] However, even though the noncovalent attachment does not alter the structure of the SWNTs, the interactions between the wrapping molecule and the nanotube are weak. Therefore if a nanocomposite of this kind was prepared, the low load transfer efficiency between the SWNT and polymer matrix would be problematic. Additionally, only specific classes of polymers can be attached onto SWNTs with these strategies.

On the other hand, a much stronger interaction between SWNTs and a polymer might be achieved by covalent functionalization. Significantly, several covalent functionalization strategies were studied recently, including fluorination with elemental fluorine;[33] ozonation;[34] cycloaddition with nitrene, carbene, or radicals;[35] Bingel reaction;[36] and electrochemical reduction of diazonium salts.[37] After being functionalized using one of these strategies, the SWNTs can then be grafted to some polymers, with their tailored chemical and surface properties, to prepare polymer−SWNT nanocomposites.[38,39]

(12) Mariwala, R. K.; Foley, H. C. *Ind. Eng. Chem. Res.* **1994**, *33*, 2314−2321.
(13) Hishiyama, Y.; Inagaki, M.; Kimura, S.; Yamada, S. *Carbon* **1974**, *12*, 249−254
(14) Acharya, M.; Raich, B. A.; Foley, H. C.; Harold, M. P.; Lerou, J. J. *Ind. Eng. Chem. Res.* **1997**, *36*, 2924−2930.
(15) Shiflett, M. B.; Foley, H. C. *Science* **1999**, *285*, 1902−1905.
(16) Rajagopalan R.; Ponnaiyan, A.; Mankidy, P. J.; Brooks, A. W.; Yi, B.; Foley, H. C. *Chem. Commun.* **2004**, *21*, 2498−2499.
(17) Qian, D.; Dickey, E. C.; Andrews, R.; Rantell, T. *Appl. Phys. Lett.* **2000**, *76*, 2868−2870.
(18) Lourie, O.; Wagner, H. D. *Compos. Sci. Technol.* **1999**, *59*, 975−977.
(19) Cooper, C. A.; Cohen, S. R.; Barber, A. H.; Wagner, H. D. *Appl. Phys. Lett.* **2002**, *81*, 3873−3875.
(20) Thess, A.; Lee, R.; Nikolaev, P.; Dai, H. J.; Petit, P.; Robert, J.; Xu, C. H.; Lee, Y. H.; Kim, S. G.; Rinzler, A. G.; Colbert, D. T.; Scuseria, G. E.; Tomanek, D.; Fischer, J. E.; Smalley, R. E. *Science* **1996**, *273*, 483−487.
(21) Girifalco, L. A.; Hodak, M.; Lee, R. S. *Phys. Rev. B* **2000**, *62*, 13104−13110.
(22) Ausman, K. D.; Piner, R.; Lourie, O.; Ruoff, R. S.; Korobov, M. *J. Phys. Chem. B* **2000**, *38*, 8911−8915.
(23) Shi, Z.; Lian, Y.; Zhou, X.; Gu, Z.; Zhang, Y.; Iijima, S.; Gong, Q.; Li, H.; Zhang, S.-L. *Chem. Commun.* **2000**, 461−462.
(24) Bahr, J. L.; Mickelson, E. T.; Bronikowski, M. J.; Smalley, R. E.; Tour, J. M. *Chem. Commun.* **2001**, 193−194.
(25) Stephan, C.; Nguyen, T. P.; de la Chappelle, M. L.; Lefrant, S.; Journet, C.; Bernier, P. *Synth. Met.* **2000**, *108*, 139−149.
(26) Curran, S. et al. *Synth. Met.* **1999**, *103*, 2559−2562.
(27) Feng, W.; Bai, X. D.; Lian, Y. Q.; Liang, J.; Wang, X. G.; Yoshino, K. *Carbon* **2003**, *41*, 1551−1557.
(28) Park, C.; Ounaies, Z.; Watson, K. A.; Crooks, R. E.; Smith, J., Jr.; Lowther, S. E.; Connell, J. W.; Siochi, E. J.; Harrison, J. S.; St. Clair, T. L. *Chem. Phys. Lett.* **2002**, *364*, 303−308.
(29) (a) Lin, Y.; Zhou, B.; Fernanado, K. A. S.; Liu, P.; Allard, L. F.; Sun, Y. P. *Macromolecules* **2003**, *36*, 7199−7204. (b) Hill, D. E.; Lin, Y.; Rao, A. M.; Allard, L. F.; Sun, Y. P. *Macromolecules* **2002**, *35*, 9466−9471. (c) Hill, D. E.; Lin, Y.; Allard, L. F.; Sun, Y. P. *Int. J. Nanosci.* **2002**, *1*, 213−221.
(30) O'Connell, M. J.; Boul, P.; Ericson, L. M.; Huffman, C.; Wang, Y. H.; Haroz, E.; Kuper, C.; Tour, J.; Ausman, K. D.; Smalley, R. E. *Chem. Phys. Lett.* **2001**, *342*, 265−271.
(31) Star, A.; Steuerman, D. W.; Heath, J. R.; Stoddart, J. F.; *Angew. Chem., Int. Ed.* **2002**, *41*, 2508−2512.
(32) Bandyopadhyaya, R.; Nativ-Roth, E.; Regev, O.; Yerushlmi-Rozen, R. *Nano Lett.* **2002**, *2*, 25−28.
(33) Mickelson, E. T.; Huffman, C. B.; Rinzler, A. G.; Smalley, R. E.; Hauge, R. H.; Margrave, J. L. *Chem. Phys. Lett.* **1998**, *296*, 188−194.
(34) Banerjee, S.; Wong, S. S. *J. Phys. Chem. B* **2002**, *106*, 12144−12151.
(35) (a) Holzinger, M.; Vostrowsky, O.; Hirsch, A.; Hennrich, F.; Kappes, M.; Weiss, R.; Jellen, F. *Angew. Chem., Int. Ed.* **2001**, *40*, 4002−4005. (b) Kamaras, K.; Itkis, M. E.; Hu, H.; Zhao, B.; Haddon, R. C. *Science* **2003**, *301*, 1501−1501. (c) Georgakilas, V.; Kordatos, K.; Prato, M.; Guldi, D. M.; Holzinger, M.; Hirsch, A. *J. Am. Chem. Soc.* **2002**, *124*, 760−761.
(36) Coleman, K. S.; Beiley, S. R.; Fogden, S.; Green, M. L. H. *J. Am. Chem. Soc.* **2003**, *125*, 8722−8723.
(37) (a) Dyke, C. A.; Tour, J. M. *J. Am. Chem. Soc.* **2003**, *125*, 1156−1157. (b) Hudson, J. L.; Casavent, M. J.; Tour, J. M. *J. Am. Chem. Soc.* **2004**, *126*, 11158−11159. (c) Bahr, J. L.; Yang, J.; Kosynkin, D. V.; Bronikowski, M. J.; Smalley, R. E.; Tour, J. M. *J. Am. Chem. Soc.* **2001**, *123*, 6536−6542. (d) Price, B. K.; Hudson, J. L.; Tour, J. M. *J. Am. Chem. Soc.* **2005**, *127*, 11867−11870.
(38) (a) Yao, Z.; Braidy, N.; Botton, G. A.; Adronov, A. T. *J. Am. Chem. Soc.* **2003**, *125*, 16015−16024. (b) Li, H. M.; Cheng, F.; Duft, A. M.; Adronov, A. *J. Am. Chem. Soc.* **2005**, *127*, 14518−14524.
(39) Buffa, F.; Hu, H.; Resasco, D. E. *Macromolecules* **2005**, *38*, 8258−8263.

Scheme 1. Preparation of SA-SWNT

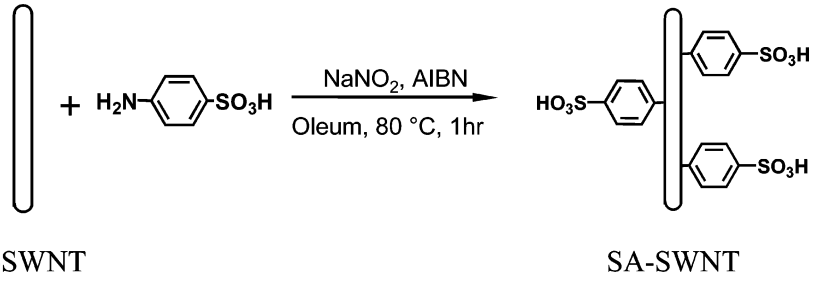

Scheme 2. Preparation of PFA-SWNT and NPC/SWNT Composite

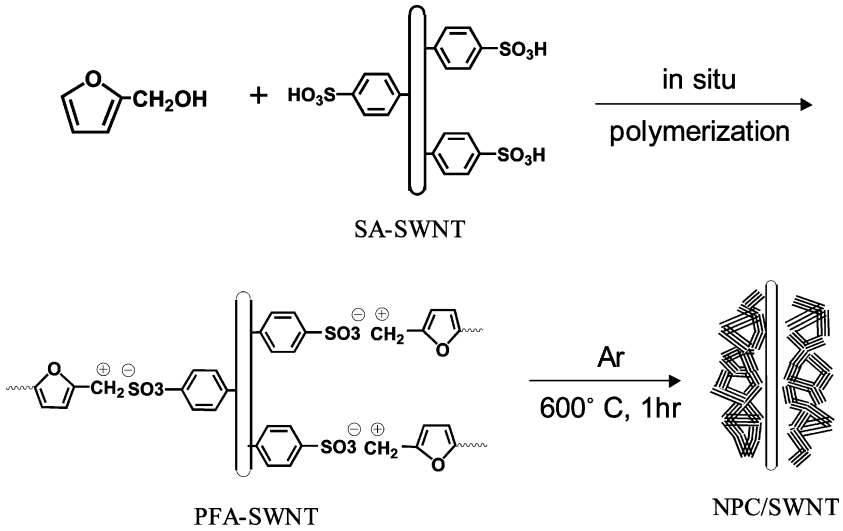

Since PFA is a cross-linking polymer,[40] it would be difficult to wrap it around an SWNT simply through noncovalent interactions. However, through covalent interactions it would be possible for PFA to bond directly with the SWNTs and to wrap them. Sulfonic acids, such as *para*-toluenesulfonic acid (*p*-TSA), are commonly used as catalyst for FA polymerization, and they have good solubility in both FA and PFA.[41] So it can be expected that an SWNT with pendant sulfonic acid groups should be dispersible in FA and should catalyze FA polymerization. Now quite conveniently for testing this line of reasoning, SWNTs with arylsulfonic acid groups may be obtained through the use of a diazonium salt functionalization methodology developed by Tour et al.[37] Based on these ideas, we report herein a method to prepare an SWNT and NPC nanocomposite. In this process, SWNTs made from high-pressure CO disproportionation (HiPco) are functionalized with an arylsulfonic acid (SA-SWNT, Scheme 1), which is similar to *p*-TSA with a methyl group substituted by an SWNT. The "grafting-to" process begins when the monomer, FA, is polymerized by the SA-SWNTs dispersed within it to produce PFA grafted to these tubes (PFA-SWNT, Scheme 2). A carbon−carbon nanocomposite was then obtained by simple pyrolysis of the PFA-SWNT. Characterization of the grafted PFA-SWNTs and the nanocomposite carbon is presented and discussed.

Results and Discussions

PFA Functionalized SWNT. HiPco SWNT purchased from Carbon Nanotechnologies, Inc. (Houston, TX) was used to prepare PFA-functionalized SWNTs. Typically a raw sample of as-prepared SWNTs (AP-SWNTs) contains metal catalyst particles surrounded by multilayer carbon shells. To remove the impurities a procedure similar to that of Smalley's group was used.[42] The purified SWNTs (p-SWNTs) were then functionalized in oleum (20% free SO_3) using sulfanilic acid, sodium nitrite, and 2,2′-azobisisobutyronitrile to produce the sulfonic acid functionalized tubes (SA-SWNTs).[37b] High-resolution transmission electron microscopy (HRTEM) images of SA-SWNTs show that the bundles become much smaller and the number of isolated SWNTs increases after functionalization (see Supporting Information).

In a typical experiment for the preparation of PFA-functionalized SWNTs, a specific amount of SA-SWNTs was dispersed in FA with an ultrasonic processor (PGC Scientifics, 130 W). To reduce spontaneous thermal polymerization, 50% of the maximum amplitude was applied and the reaction was kept in an ice bath. After ultrasonicating for 5 h, the suspension was poured into water with 10 times the volume of the FA. The first thing that could be noticed about these SA-SWNTs was the change in their water solubility (Figure 1). Due to the hydrophilic nature of the sulfonic acid group, SA-SWNTs were water-soluble and the solution is dark; however, after being treated with FA (PFA-SWNTs), they became insoluble and the solution is clear with the nanotubes lying at the bottom of the vessel. Since FA is miscible with water, the insolubility of the PFA-SWNTs in water is due to the formation of PFA on the tube, since the PFA is quite hydrophobic.

(40) Choura, M.; Belgacem, N. M.; Gandini, A. *Macromolecules* **1996**, *29*, 3839−3850.
(41) Principe, M.; Ortiz, P.; Martinez, R. *Polym. Int.* **1999**, *48*, 637−641.
(42) Chiang, I. W.; Brinson, A. Y.; Willis, P. A.; Bronikowski, M. J.; Margrave, J. L.; Smalley, R. E.; Hauge, R. H. *J. Phys. Chem. B* **2001**, *105*, 8297−8301.

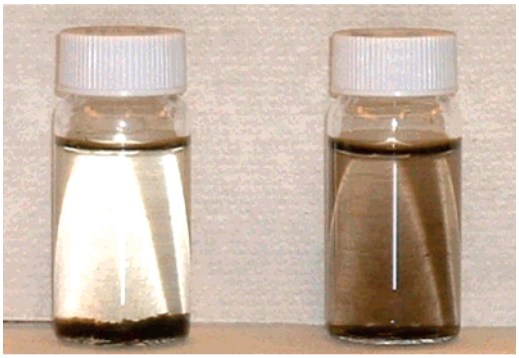

Figure 1. Photograph of SWNTs in water. (a) PFA-SWNT with a clear supernatant and precipitate versus (b) SA-SWNT with a dark supernatant due to dispersion and solubility.

Contact angles of water on a membrane of an SA-SWNT versus on a membrane of a PFA-SWNT were measured to confirm that a transition from hydrophilic to hydrophobic had occurred on SA-SWNTs after being treated with FA. For this objective, membranes of SA-SWNTs and PFA-SWNTs were prepared by casting them from a water suspension onto a 0.2 μ Anodisc filter membrane. The membrane of the PFA-SWNT was washed thoroughly with water and acetone repeatedly to remove monomer FA and unattached PFA. The contact angle of water on the membrane of the SA-SWNT was ~40°. The membrane of the PFA-SWNT was definitely hydrophobic with a much higher water contact angle of $90 \pm 5°$. Scanning electron microscopy (SEM) images were taken of both membranes (Figure 2). The morphology remains almost the same for SA-SWNTs and PFA-SWNTs. Bundles of SWNTs could be seen on both membranes without obvious size changes. The images of the washed PFA-SWNT membrane confirmed that the hydrophobic character did not arise through a simple covering of the nanotube mat by bulk PFA thereby changing the contact angle. These results indicated that polymer was formed on the surface of the SWNT after FA treatment and that the polymer was strongly bonded with the SWNT because it could not be removed even after extensive washing and filtration.

The membrane of the PFA-SWNT was vacuum-dried and peeled off from the Anodisc filter membrane to obtain an isolated product. Raman and FTIR spectra were taken to characterize it.

Raman spectra were obtained with an excitation wavelength of 514.5 nm (Figure 3). The spectra appear in two panels: 100−400 cm^{-1} and 1250−1800 cm^{-1}. In the Raman spectrum of SWNTs, the band in the range 150−300 cm^{-1} is attributed to the radial breathing mode (RBM) of the SWNT. The frequency of the RBM varies inversely with the nanotube diameter d.[43] In the high-frequency region of 1250−1800 cm^{-1}, there are two bands that are associated with the tangential C−C stretching modes of the SWNTs. The stronger band around 1590 cm^{-1} is close to that of well-ordered graphite, i.e., the E_{2g} band at 1582 cm^{-1}, so it is called the G band. The G band of an SWNT is associated with its ordered sp^2 hybridized carbon network. The weak band at ~1300 cm^{-1}, the so-called D band, involves the scattering of an electron via phonon emission by the disordered sp^2 network. Usually, the intensity of the D band is used to probe the degree of functionalization. Any change on the nanotube wall that affects its periodicity may strengthen the D band scattering. It may arise from missing C atoms (vacancies), covalent bond formation, or disorder of any kind in the aromatic π-domain. It is clear that the D band intensity of SWNTs has significantly increased after being functionalized with the sulfonic acid group (Figure 3B). The Raman spectrum of the PFA-SWNT (Figure 3C) has similar features to those of the SA-SWNT in both RBM and tangential mode. The intensity ratio of the D band to G band (I_D/I_G) was almost the same as that of the SA-SWNT, suggesting that PFA wrapping did not alter the hybridization of the carbon atoms within the SWNT framework. It was consistent with Scheme 2, in which the PFA was only attached on the end of the sulfonic acid group. It was also observed that the RBM of the PFA-SWNT became even weaker than that of the SA-SWNT. This would be expected if the attachment of the macromolecule would restrict the radial breathing of SWNTs more than the arylsulfonic acid group alone, a conclusion which seems logical.

IR spectroscopy is useful for identifying the functional groups appended to the SWNTs.[44] Figure 4 shows the IR spectra of p-SWNT (A), SA-SWNT (B), and the PFA-SWNT (C). The large IR band observed at ca. ~3400 cm^{-1} was attributed to asymmetrical stretching vibrations of traces of water adsorbed in the KBr pellet used for the analysis. The aromatic C═C stretch at 1627 cm^{-1} is commonly seen in IR spectra of SWNTs. After functionalization, new bands at 1081 and 1045 cm^{-1} appeared which corresponded to the sulfonic acid group. It was interesting to note that the bands for the PFA-SWNT shifted to lower frequencies by about 10 wavenumbers compared with the SA-SWNT. This clearly suggested that there could be electrostatic attractions between the sulfonic acid groups and the growing chains of PFA. The new signal at 1112 cm^{-1} was from the ether linkage in PFA, which is proof of FA polymerization. Enhancement of the C−H stretching mode at 2922 and 2853 cm^{-1} also confirmed the existence of PFA.

NPC/SWNT Nanocomposite Carbon. A PFA-SWNT was pyrolyzed in Ar at 600 °C for 1 h to obtain the NPC/SWNT nanocomposite. For comparison, an SA-SWNT was also treated under the same conditions. Upon heating, PFA wrapped around the SA-SWNT was converted into NPC. The resulting NPC/SWNT nanocomposite was characterized with HRTEM and Raman.

The Raman spectrum of the NPC/SWNT nanocomposite showed strong RBMs (Figure 3E), as did the p-SWNT and the annealed SA-SWNT (Figure 3D). Although wrapped with PFA, the heat treatment in inert gas could still cleave the arylsulfonic acid group from the SA-SWNT to restore the spectroscopic signature of the p-SWNT. The restoration of the RBMs means that the SWNTs are intact after ultrasonication and even after pyrolysis. But upon closer observation of the Raman spectrum of the NPC/SWNT nanocomposite, slight shifts to higher wavenumbers are found in all the RBMs. Since the RBMs of the NPC/SWNT nanocomposite have intensities comparable to those of the p-SWNT, we may assume there is no chemical bonding or charge transfer between the SWNT and NPC and attribute these shifts to molecular force being exerted by the

(43) Rao, A. M.; Richter, E.; Bandow, S.; Chase, B.; Eklund, P. C.; Williams, K. A.; Fang, S.; Subbaswamy, K. R.; Menon, M.; Thess, A.; Smalley, R. E.; Dresselhaus, G.; Dresselhaus, M. S. *Science* **1997**, *275*, 187.

(44) Kim, U. J.; Furtado, C. A.; Liu, X.; Chen, G.; Eklund, P. C *J. Am. Chem. Soc.* **2005**, *127*, 15437−15445.

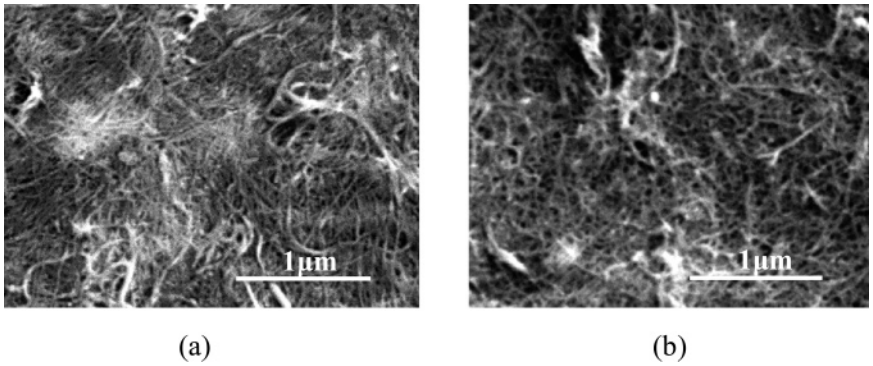

Figure 2. SEM image of membrane of SA-SWNT (a) and PFA-SWNT (b).

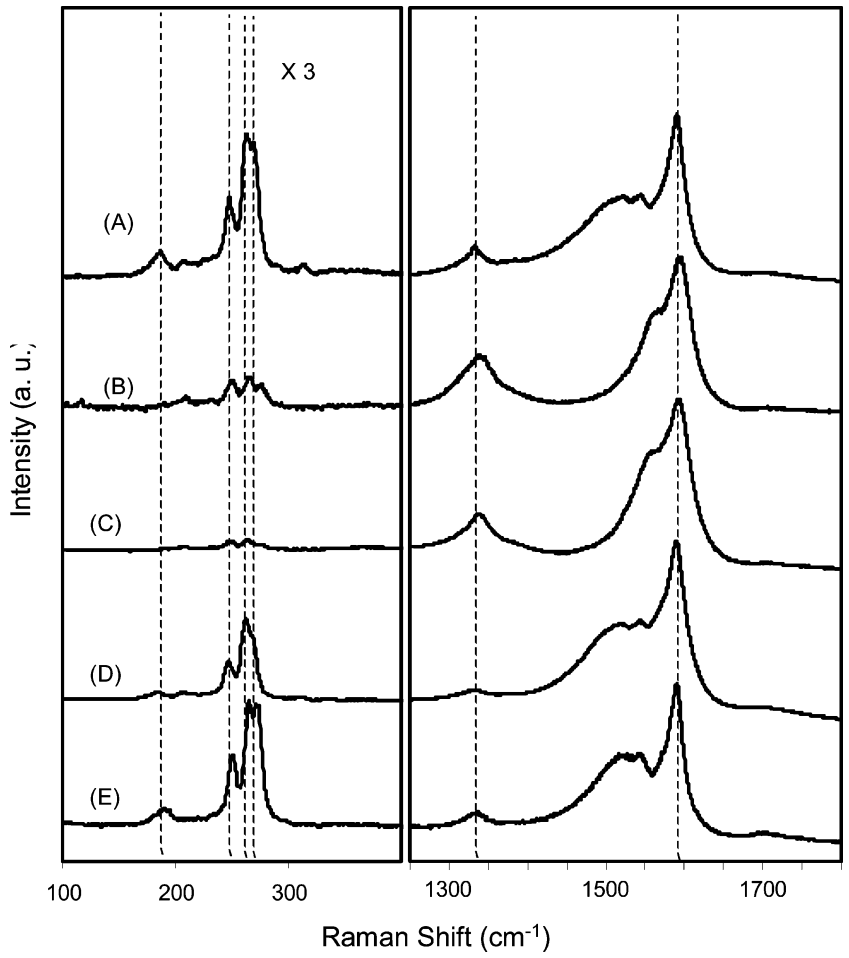

Figure 3. Raman spectra of p-SWNT (A), SA-SWNT (B), PFA-SWNT (C), SA-SWNT annealed in Ar at 600 °C for 1 h (D) and NPC/SWNT nanocomposite carbon (E). For comparison, all of the spectra were normalized with the strongest tangential band, and all of the RBMs were enhanced by a factor of 3.

NPC on the SWNT. It has been well established that there is an upshift in Raman scattering of SWNT bundles under high pressure.[45] Therefore, it can be calculated that the molecular pressure of the NPC on the SWNT is hundreds of MPa based on RBM shifts. It is also interesting to notice that bigger tubes have more shift than the smaller tubes. In the RBM of the NPC/SWNT nanocomposite, the three bands of the p-SWNT at 247, 262, and 269 cm^{-1} have shifts of $\sim$3 cm^{-1}, while the band at 186 cm^{-1} shifts by $\sim$5 cm^{-1}. This is consistent with literature, considering that RBM frequency is diameter dependent.[45b] Although there is an obvious frequency change in RBMs, tangential modes remain at almost the same frequency. We attribute this to the anisotropic behavior of the NPC on the SWNT. When PFA was pyrolyzed to the NPC, there is considerable volume shrinkage in all dimensions, which may induce compressive stress on the SWNT. The compressive stress affects the SWNT more radially than tangentially. In other words, there is hoop stress on the SWNT from pyrolysis of the

(45) (a) Venkateswaran, U. D.; Rao, A. M.; Richter, E.; Menon, M.; Rinzler, A.; Smalley, R. E.; Eklund, P. C. *Rhys. Rev. B* **1999**, *59*, 10928−10934. (b) Venkateswaran, U. D.; Brandsen, E. A.; Schlecht, U.; Rao, A. M.; Tichter, E.; Loa, I.; Syassen, K.; Eklund, P. C. *Phys. Status Solidi B* **2001**, *223*, 225−236. (c) Wood, J. R.; Zhao, Q.; Frogley, M. D.; Meurs, E. R.; Prins, A. D.; Peijis, T.; Dunstan, D. J.; Wagner, H. D. *Rhys. Rev. B* **2000**, *62*, 7571−7575. (d) Merlen, A.; Toulemonde, P.; Bendiab, N.; Aouizerat, A.; Sauvajol, J. L.; Montagnac, G.; Cardon, H.; Petit, P.; Miguel, A. S. *Phys. Status Solidi B* **2006**, *243*, 690−699.

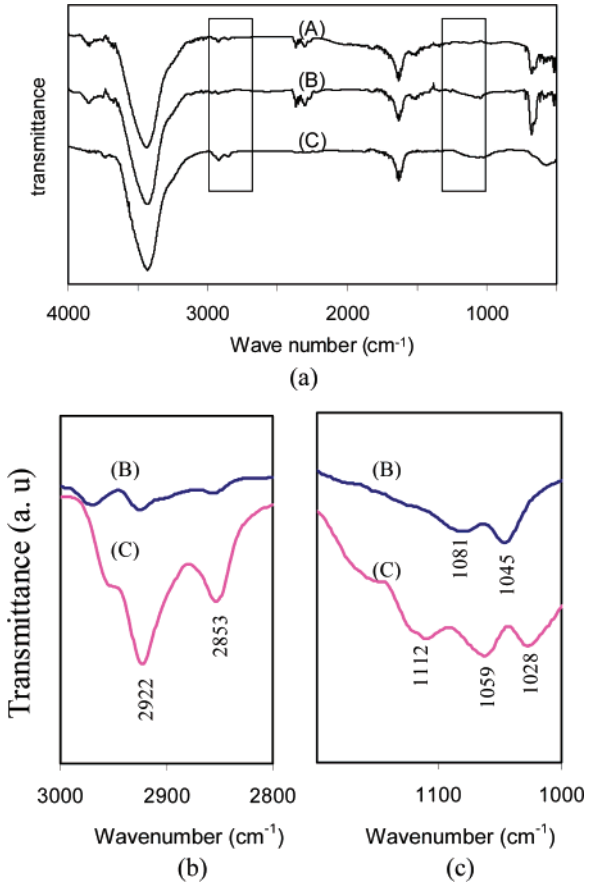

Figure 4. (a) IR spectra of p-SWNT (A), SA-SWNT (B), and PFA-SWNT (C); (b) expanded region of 3000−2800 cm^{-1}, highlighting the enhancement of C−H stretch; and (c) expanded region of 1200−1000 cm^{-1}, showing appearance of ether linkage and shift of sulfonic acid group stretch.

NPC. This can explain the upshift observed in the RBM. In the tangential mode of the NPC/SWNT nanocomposite, we also found that it has a slightly stronger D band than that of the annealed SA-SWNT. Although the NPC compared with the SWNT had a higher I_D/I_G, the absolute tangential mode intensity was much lower. Hence, when the amounts of the NPC and SWNT are comparable in the composite, the NPC component contributes little to the overall tangential mode of the composite. Although the exact concentration of the NPC cannot be measured directly, the approximate weight ratio of the NPC to SWNT can be obtained by the weight change in the synthesis process of the NPC/SWNT nanocomposite. Usually, this ratio is from 1:1 to 2:1 in the nanocomposite prepared with the method described above. So the D band increase could not be attributed to the existence of the NPC only. Actually, when the PFA-SWNT was pyrolyzed, there was volume shrinkage of the PFA, which will cause stress between the NPC and the SWNT. This stress will disrupt the symmetry of the graphene plane. Therefore it is more likely that the small enhancement in the D band intensity is caused by the interaction between the NPC and SWNT.

The NPC/SWNT nanocomposite retains the thin bundle structure similar to that of the SA-SWNT as shown in the HRTEM images (Figure 5). A high magnification image of the NPC/SWNT nanocomposite reveals that SWNTs are covered with some amorphous carbon. The morphology of this amorphous carbon looks the same as that of the NPC pyrolyzed from

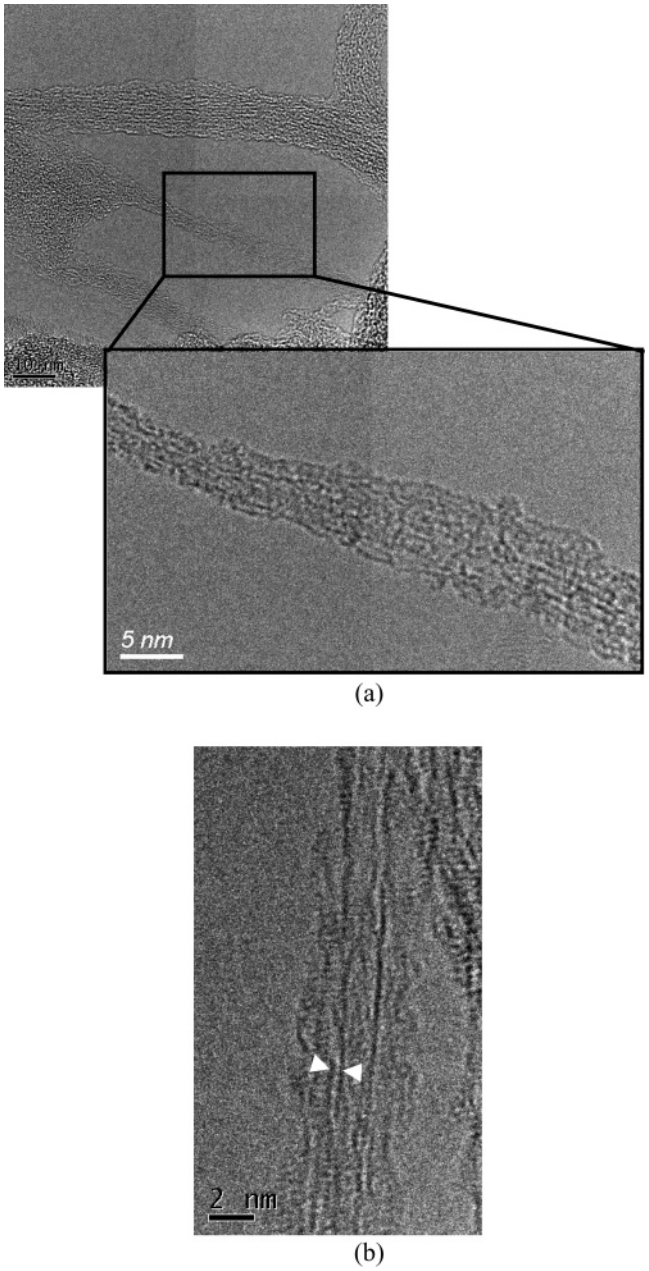

Figure 5. HRTEM of SWNT/NPC nanocomposite. (a) SWNT bundles covered with NPC and (b) individual SWNT surrounded with NPC, with the white triangles pointing to the gap between NPC and SWNT.

PFA only.[46] In another image showing an individual SWNT (Figure 5b), it can be seen that there is a gap of 3−4 Å between the NPC and the SWNT. This suggests strong van der Waals interaction rather than covalent bonding between the two components. It is consistent with the hypothesis made based upon the Raman spectra. It was also observed that the orientation of the carbon sheet close to the SWNT was along the tube axis. It suggests that the SWNT may template the NPC within a short range. All of these images imply that a continuous phase was formed between these two distinct types of carbon. Thus the preparation of a nanocomposite carbon with an SWNT becomes possible by modifying the SWNT with a carbonizable polymer.

(46) Aso, H.; Matsuoka, K.; Sharma, A.; Tomita, A. *Carbon* **2004**, *42*, 2963−2973.

Conclusion

A novel nanocomposite carbon was prepared based on grafting a carbonizable polymer to SWNTs. The SWNTs were functionalized with a sulfonic acid group, which acted as a catalyst for furfuryl alcohol (FA) polymerization, allowing the formation of poly(furfuryl alcohol) (PFA)-functionalized SWNTs (PFA-SWNTs). Contact angle measurements and SEM images showed that the surface properties of the SWNTs were changed after being treated with FA. The infrared spectrum provided further evidence of formation of PFA and electrostatic attraction between the sulfonic acid group and PFA. The formation of PFA-SWNTs provided a way of overcoming the inherently low interaction between pure SWNTs and the carbon precursor. Pyrolysis of the PFA-SWNT produced a nanocomposite carbon with the NPC covering the SWNT. This procedure leads to intimate contact between the NPC and SWNT without affecting the integrity of the SWNT. A continuous phase is formed between the NPC and the SWNT which prevents the segregation of the SWNT from the NPC matrix. This suggests potential application of the PFA-functionalized SWNT in the preparation of advanced C/C nanocomposites.

Experimental Section

Materials. HiPco-produced single-wall carbon nanotubes (SWNTs) were purchased from Carbon Nanotechnologies, Inc. (Houston, TX). HCl (36.5 wt %), oleum (20% free SO_3, A.C.S regent), sodium nitrite (99.99+%, RegentPlus), sulfanilic acid (99% A.C.S regent), 2,2′-azobisisobutyronitrile (98% A.C.S regent), and furfuryl alcohol (99%) were purchased from Sigma-Aldrich (Allentown, PA). Polycarbonate track-etch membranes (0.2 μ, Whatman Nuclepore) and Anodisc filter membranes (0.2 μ, Whatman Anodisc) were from Fisher Scientific (Pittsburgh, PA).

Purification of SWNTs. AP-SWNTs (100 mg) were put in a tube furnace for wet oxidation. Air passing through a water bubbler at room temperature was flowed into the furnace tube at a flow rate of 200 sccm. The SWNTs were heated to 225 °C and kept at this temperature for 18 h. Then it was dispersed in 50 mL of concentrated HCl in a 100 mL flask by ultrasonicating for 1 h followed by stirring and refluxing at 60 °C for 18 h. Finally, the SWNTs were heated in Ar at 800 °C for 1 h.

Functionalization of SWNTs. Purified SWNTs (50 mg, p-SWNT) were stirred in 50 mL of oleum in a 100 mL flask for 3 h. Then they were heated to 80 °C, and 1.15 g sodium nitrite (4 equiv/mol C), 2.886 g sulfanilic acid (4 equiv/mol C), and 0.137 g AIBN, (0.2 equiv/mol C) were added. Kept at 80 °C and stirred for 1 h, the mixture was poured *slowly* and *carefully* into more than 500 mL of water and filtered through a 0.2 μ track-etch membrane. The filter cake was washed with acetone and water repeatedly. Then it was vacuum-dried at 100 °C overnight, and SA-SWNTs were collected.

Synthesis of PFA-SWNTs. SA-SWNTs (5 mg) were dispersed in 10 mL of FA in a 20 mL vial with a 6 mm ultrasonic probe of the ultrasonic processor (PGC Scientifics, 130 W). The vial was kept in an ice bath. Cycles of 5 s pulses following 5 s of ultrasonication were used. After 5 h of ultrasonication, the mixture was poured in 100 mL of water and filtered with a 0.2 μ Anodic membrane. The filter cake was washed with acetone and water repeatedly and vacuum-dried at room temperature.

Synthesis of the SWNT/NPC Nanocomposite. PFA-SWNTs (5 mg) were heated to 600 °C with a heating rate of 10 °C/min and soaked for another 1 h under flowing argon.

Annealing of SA-SWNTs. SA-SWNTs (10 mg) were put in a tube furnace and heated to 600 °C with a heating rate of 10 °C/min and kept for 1 h under flowing argon.

Characterization. p-SWNTs and SA-SWNTs were dispersed in ethyl alcohol with an ultrasonic processor to make a suspension. The NPC/SWNT nanocomposite was ground in an agate mortar followed by dispersing with ethyl alcohol. HRTEM samples were made by dropping the suspensions on the holey carbon-coated grids. HRTEM images were taken with a JEOL 2010F operating at 200 kV. The point-to-point resolution was ~2 Å. Raman spectra were collected under ambient conditions with a Jabin-Yvon Horiba T64000 micro Raman spectrometer. Excitation was provided by an Ar−Kr laser at 1−3 mW incident power. SEM images were taken with Hitachi S-3000H operating at 5 kV. Both SA-SWNT and PFA-SWNT membranes were sputtered with gold before characterization. Contact angles were measured with a contact angle goniometer equipped with a CCD camera. Infrared spectra were taken using a Nexus 670 FT-IR spectrometer. The samples were mixed with KBr and palletized. The measurements were done in transmission mode.

Acknowledgment. This project is funded by NSF NIRT DMR01-03585. The authors would like to thank Krishna Dronavajjala for contact angle measurements. We would also like to thank Dr. Joe Kulik for help in HRTEM. P.C.E. acknowledges support from the NSF NIRT program.

Supporting Information Available: HRTEM image of the SA-SWNT. The photos of water contact angle measurements. Complete ref 26. This material is available free of charge via the Internet at http://pubs.acs.org.

JA063518X